80/21

EISCAT
TECHNICAL
NOTE

EISCAT VHF ANTENNA TESTS

by
Per-Simon Kildal

KIRUNA
Sweden

EISCAT VHF ANTENNA TESTS

by

Per-Simon Kildal

EISCAT Technical Note 80/21
EISCAT Scientific Association
Printed in Sweden
Kiruna, September 1980
ISSN 0349-2710

EISCAT VHF ANTENNA TESTS

by

Per-Simon Kildal

Abstract

The report contains the main results of the measurements on the EISCAT VHF antenna during the RF acceptance tests in December 1979 and March 1980.

The VHF antenna satisfies all specifications with adequate margins at broadside and for phase steering angles up to 21.3^{o}. However, phase steering angles larger than 21.3^{o} cannot be reached because the impedance mismatch of the vertical (i.e. transverse) dipoles increases severely.

Preface

The contract for the EISCAT VHF parabolic cylinder antenna was given to a consortium of the German companies MAN, KRUPP and MBB (Messerschmidt-Bölkow-Blohm) in February 1978.

The electrical design of the antenna was done in cooporation with EISCAT. Final review of both the mechanical and electrical design took place in January 1979.

The erection of the antenna was completed during the summer and autumn 1979. Some minor adjustments and painting work was left until May 1980.

A brief breakdown of the total price of the antenna is shown in Table 1. Different ordered options are included in the prices, except spare parts.

This report contains the main results of the RF tests, both the acceptance tests proposed by MBB, and the additional tests proposed by Kildal. The tests were performed from 1 Dec. to 15 Dec. 1979, and from 26 Febr. to 20 March 1980, by Mr. Schroer and Mr. Killesreiter from MBB, Svein Olav Simonsen and Jan Henriksen from EISCAT, and Per-Simon Kildal from ELAB. The phase steering of the antenna was done by EISCAT staff under direction of Per-Simon Kildal.

Four 30m x 40m antenna elements with back skin (and incremental encoders)	DM 8 427 300.00
RF distribution system, phasing cables and optimized dipole design	DM 3 115 100.00
Switch yard	228 700.00
Foundations	DM 1 280 000.00
Total price (incl. DM 181.450,00 discount)	DM 12 640 950.00

Table 1. Breakdown of prices of VHF antenna.

Only a few drift scans of Cas A are included in this report. More scans are found in the measurement journal [10]. A discription of the measurement setup and detailed measurement results of the active reflection loss of the dipoles are found in the measurement journals [11] and [12].

CONTENTS

LIST OF DIAGRAMS

LIST OF TABLES

LIST OF FIGURES

I. SUMMARY OF RESULTS

This section contains a summary of the measurement results presented in [10], [11], [12]and Sec. II and Sec. III of this report.

I.1. Line Feed Measurements

The amplitude and phase distribution along the linear dipole array was measured [12]. The r.m.s. amplitude and phase errors was calculated from the measurement results. The results are given in Table 1, together with the insertion loss of the RF distribution system. All results are within the specifications.

Table 1. Line feed measurements [12]

Line feed measurements	Polarization	Measured	Specified
Amplitude error	HOR	0.11 dB	0.8 dB
" "	VER	0.16 dB	0.8 dB
Phase error	HOR	2.3°	5°
" "	VER	2.39°	5°
Insertion loss	HOR	0.393±0.1 dB	0.6±0.06 dB
" "	VER	0.433±0.1 dB	0.6±0.06 dB
Phase between HOR and VER pol., switch yard pos. II	Sec. 1 and 2	92.0°	$90^{\circ}\pm5^{\circ}$
	Sec. 3 and 4	92.5°	$90^{\circ}\pm5^{\circ}$

The measurement setups for these measurements are shown in [12] They are in principle as shown in fig. 7. However, the amplitudes and phases were measured with a vector voltmeter instead of the ELCOM network analyzer with built-in generator. The separate signal generator was places near the input of the RL345 line, feeding the RL345 line and the 200 m RG13/u cable running up to the feeder bridge. The 200 m RG13/u cable provided the reference signal for the vector voltmeter, which was mooved along the line feed from dipole to dipole together with the calibrated measurement cable shown in fig. 7. Then the amplitude and phase exciting

each dipole could be measured on the forward port of the directional coupler which was part of the calibrated measurement cable. In this way the phase stability was assured because the test signal through the line feed and the reference signal got nearly the same time delay.

I.2. Switch Yard

The switch yard has two positions, mode 1 and 2. Antenna mode 1 means that the antenna operates as one antenna, one RL 345 line feeding one polarization, and the other the orthogonal polarization. Antenna mode 2 means that one RL 345 line feeds the two western sections (1-2) of the antenna, and the other the two eastern sections (3-4), so that it operates as two antennas, each with circular polarization.

When the antenna is in mode 2, both halves transmit with right hand circular polarization. The back-scattered signal will have left circular polarization, and will be received on a port on a 3 dB hybrid inside the switch yard. The coupling C of the input RL345 lines to the receiver ports in the switch yard was measured. The results are (worst case at 224 MHz) [11]

C <- 25 dB at broadside
C <- 28 dB for $\theta = 21.3^{o}$
C <- 16 dB for $\theta = 25.2^{o}$

I.3. VSWR

The VSWR at the input of the RL345 line was found by measuring the return loss at the input. See Fig. 1 and 2. The specification within the ±1.25 MHz transmit band is

VSWR < 1.4

This is satisfied at broadside and for a phase steering angle $\theta = 21.3^{\circ}$ with large margins. The specification is also satisfied for $\theta = 25.2^{\circ}$. See Table 2.

Table 2. VSWR at input of RL345 line within transmit band. (224 ± 1.25 MHz)

		MODE 1		MODE 2	
		Hor.pol	Ver.pol	Sec.1-2	Sec.3-4
Broadside $\theta = 0^{\circ}$	Return loss	24 dB	26 dB	26 dB	26 dB
	VSWR	1.13	1.11	1.11	1.11
$\theta = 21.3^{\circ}$	Return loss	26 dB	30 dB	27 dB	35 dB
	VSWR	1.11	1.07	1.09	1.04
$\theta = 25.2^{\circ}$	Return loss	26 dB	16 dB	19 dB	21 dB
	VSWR	1.11	1.38	1.25	1.20

HORIZONTAL POL.

VERTICAL POL

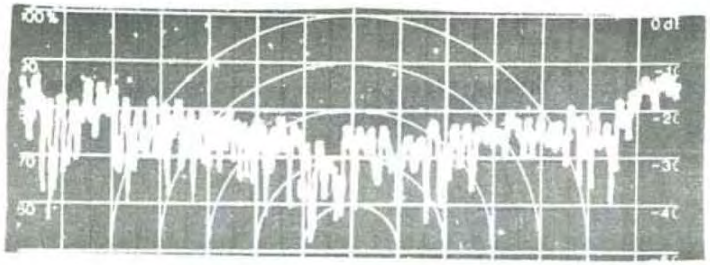

θ = 0°
N = 0

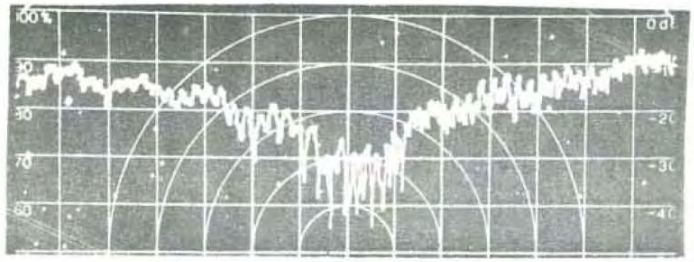

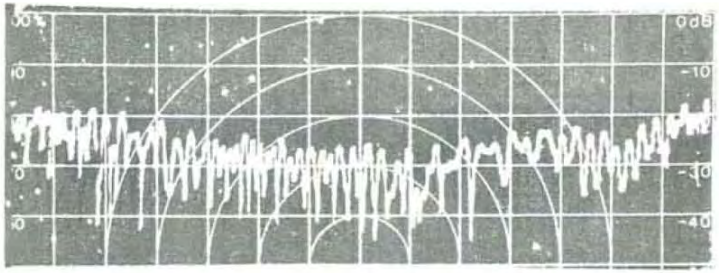

θ = 21.3°
N = 17

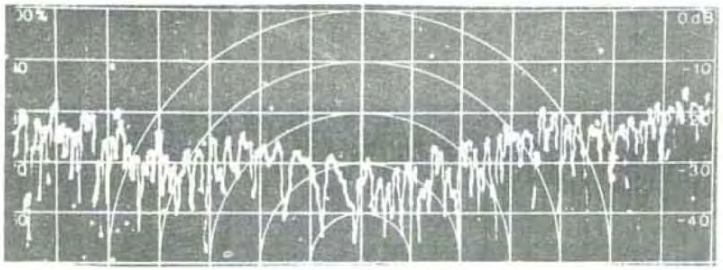

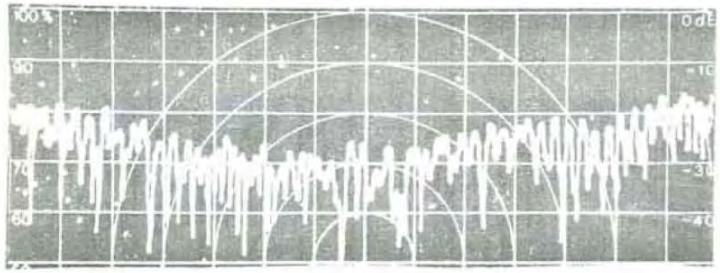

θ = 25.2°
N = 20

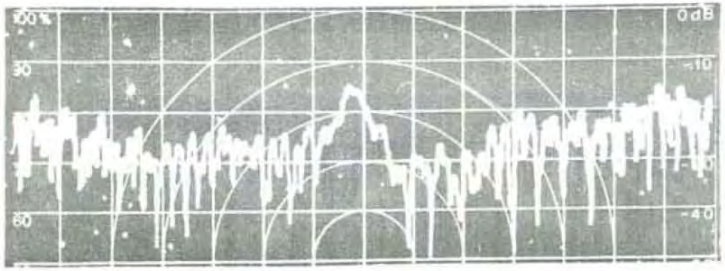

Fig. 1. Reflection level at input of RL345 line. Forward reference level is 0 dB. 10 dB/div. 5 MHz/div. The antenna operates in mode 1, i.e. as one antenna.

Antenna elements 1-2

Antenna elements 3-4

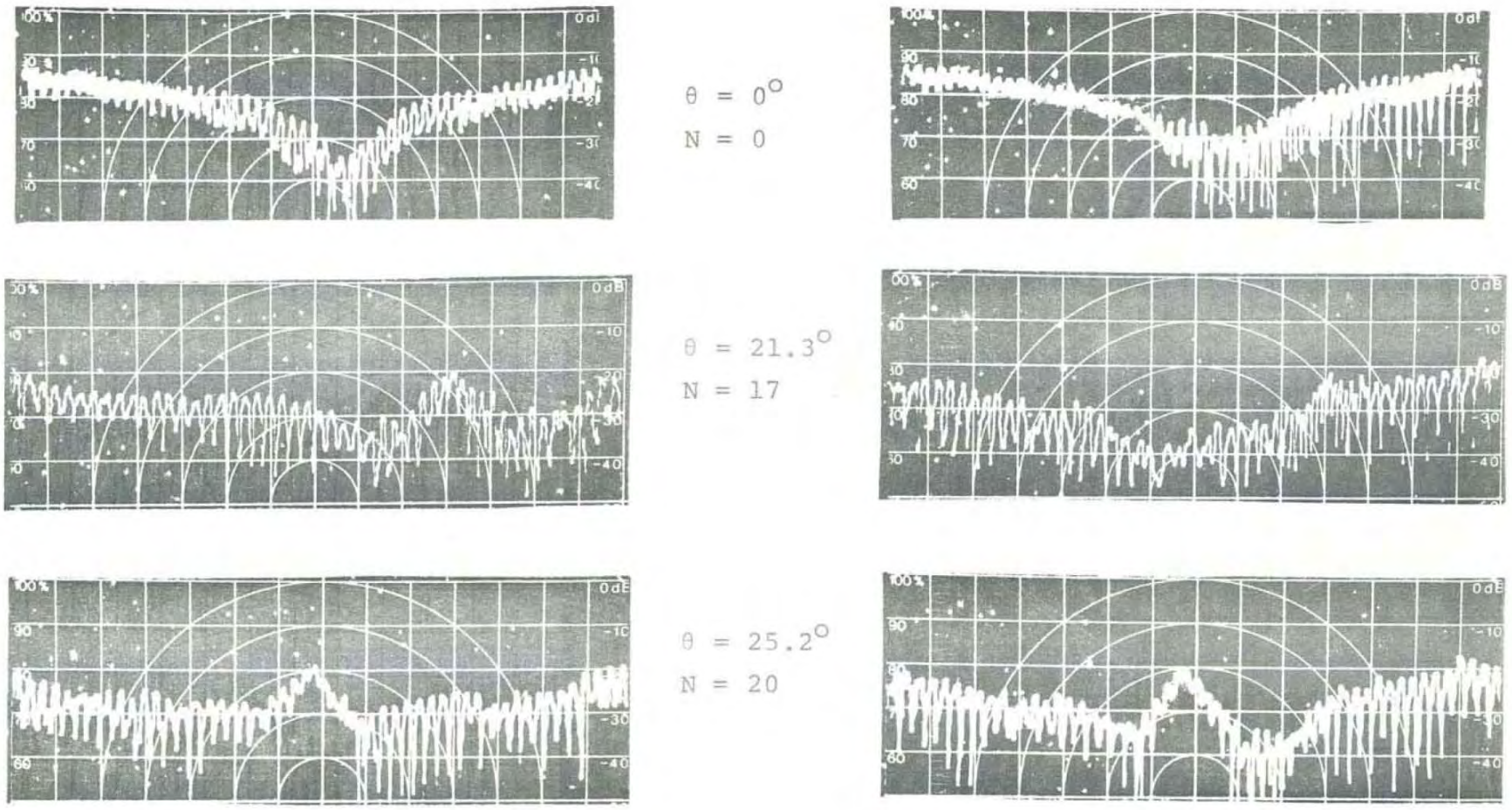

Fig. 2. Reflection level at input of RL345 line. Forward reference level is 0 dB. 10 dB/div. 5 MHz/div. The antenna operates in mode 2, i.e. as two separate antennas.

I.4. Manual Phase Steering

The VHF antenna can be phase steered manually by connecting precut 7/8" Flexwell cables to the dipoles. There are 4 groups of 67 phase cables with different length. It is possible to phase steer the antenna to 20 directions between broadside and 25.2° on either side of broadside by rearranging the sequence of phase cables that are connected to each array element [4]. The possible phase steering angles measured from broadside are given by

$$\theta_N = \arcsin\left(\frac{N}{0.7 \cdot 67}\ \frac{f_o}{f}\right) \qquad N = 1,2,---,20$$

where f_o = 224 MHz and f is the actual measurement frequency [4].

A computer program have been made in order to find the correct cables to be connected to the dipoles for a given N.

During the tests in March 1980 the complete antenna was phase steered to θ_{17} = 21.3° and θ_{20} = 25.2° at 224 MHz. Part of the antenna was phase steered to some angles between.

It takes 4 persons about 4 hours to phase steer the complete antenna from one angle to another. That is faster than expected. The phase steering is simplified because all phase cables are mounted on the wall inside the feeder bridge.

MBB once offered EISCAT 256 coaxial line stretchers instead of the phase cables, for an additional price of

a) Manually activated	416 610.- DM
b) Motor driven	593 280.- DM
c) Motor driven with control position	648 650.- DM

The cheapest of these options amounts to more than 1.1 million N.kr. For that price it is possible to phase steer the antenna manually 625 times if the 4 "phase shifters" have an hourly pay of 100 N.kr.

EISCAT requires only the beam to be phase steered between 5 and 10 times a year. The choice of manual phase steering seems, therefore, to be highly cost effective.

I.5. Dipole Impedance

The return loss at the dipole inputs with all dipoles excited with correct amplitude and phase, was measured at broadside and when phase steered, see Sec. II. The results are summarized in Fig. 3, which shows the mean transmission coefficient η_{imp} due to impedance mismatch at dipole inputs. The curves show a severe mismatch for vertical polarization for $\theta = 25^{\circ}$. Almost half the incident power is reflected by the dipole. In fact the return loss on the measured dipoles varied between 0.7 dB and 6.5 dB for this position.

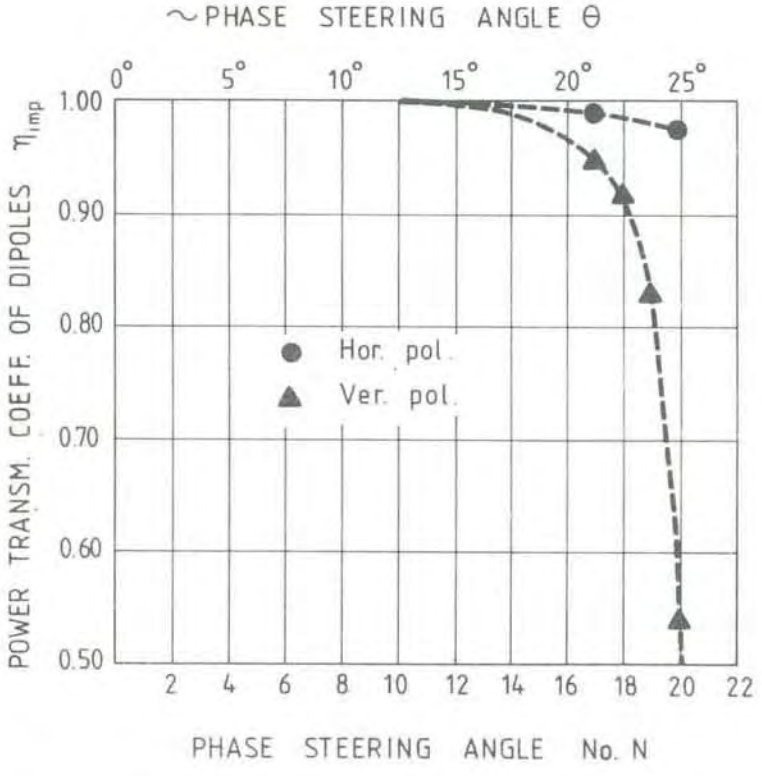

Fig.3. Efficiency due to measured impedance mismatch of dipoles. N = 20 corresponds to 25.2° and N = 17 to 21.3° phase steering angle.

The effect, which was not foreseen by either EISCAT or MBB, was explained by Mr. Liesenkötter, leader of the antenna Deparment at MBB. When the feed is phase steered to 25.2° (N=20), the phase difference between two neighbouring dipoles is

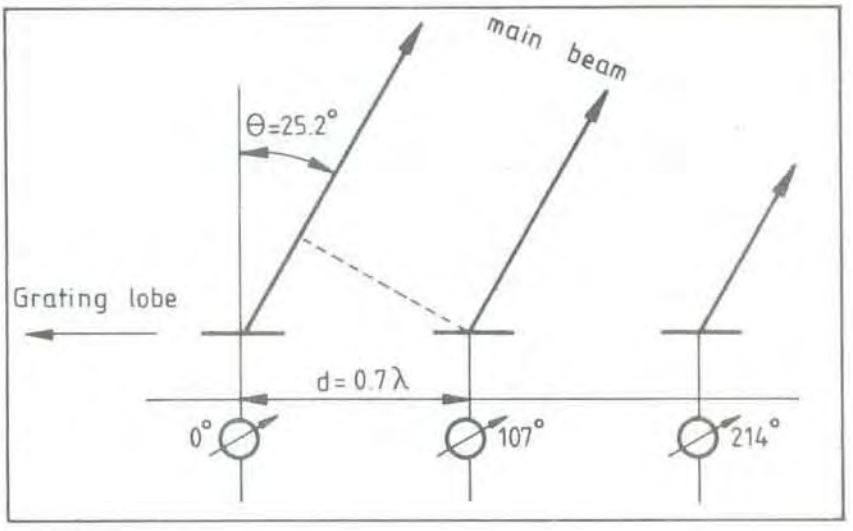

Fig.4. Phase steering, main lobe and grating lobe.

$$\Delta\phi = \frac{20}{67} \cdot 360^{\circ} = 107^{\circ}$$

The spacing between the dipoles is 0.7λ at 224 MHz, which equals 252°. Thus, a grating lobe occurs for θ=-90° because 107°+252°≈360°, but it does not radiate because the element pattern of a dipole above ground plane is zero for θ=90°. Therefore, no problems ought to occur. The spacing 0.7λ was in fact chosen so that no radiating grating lobes should occur for phase steering angles up to 25°. However, the dipoles which are normal to the array axis (referred to as transverse or vertical polarization) can excite a surface wave propagating in the direction of the grating lobe. (The surface wave is evanescent in the direction normal to the surface). It is reflected at the end of the line feed. It does not radiate significantly in the endfire direction. But the surface wave propagating back and forth along the array makes the line feed similar to a resonator. The resonance effect can be seen in the return loss curves in Fig. 5. The surface wave is only present in very long arrays. It was not seen on the 7 elements scale model measured by Kildal [9].

HORIZONTAL POLARIZATION

$\theta = 0^{\circ}$ N = 0
5 MHz/div.

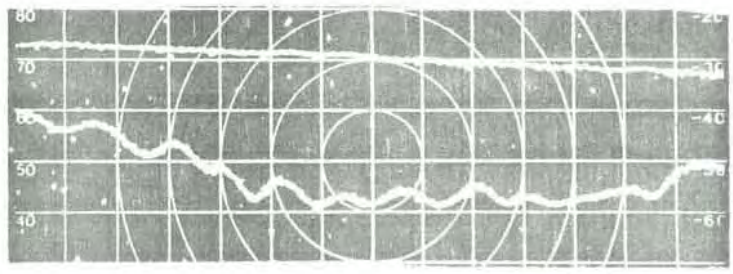

$\theta = 21.3^{\circ}$ N = 17
11/6 MHz/div.

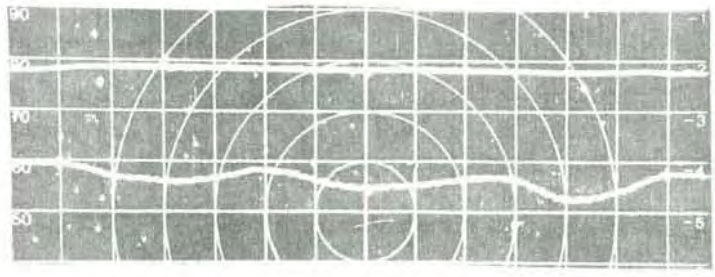

$\theta = 25.2^{\circ}$ N = 20
5 MHz/div.

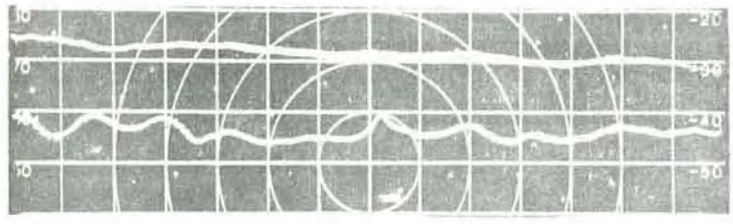

VERTICAL POLARIZATION

$\theta = 0^{\circ}$ N = 0
5 MHz/div.

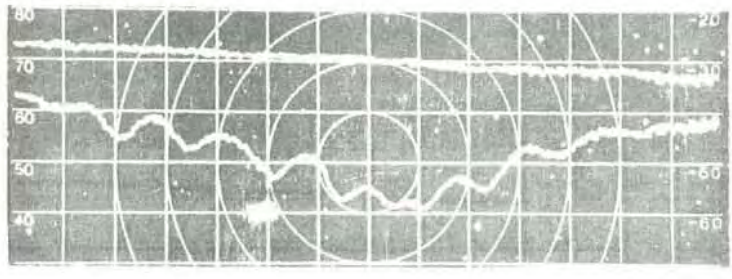

$\theta = 21.3^{\circ}$ N = 17
11/6 MHz/div.

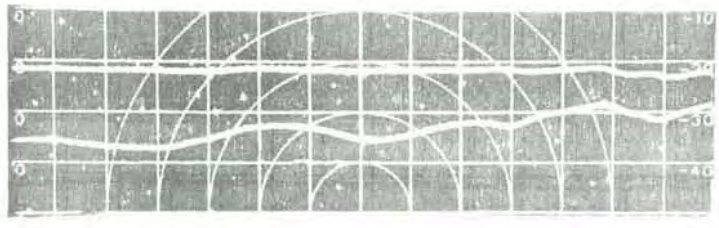

$\theta = 25.2^{\circ}$ N = 20
5 MHz/div.

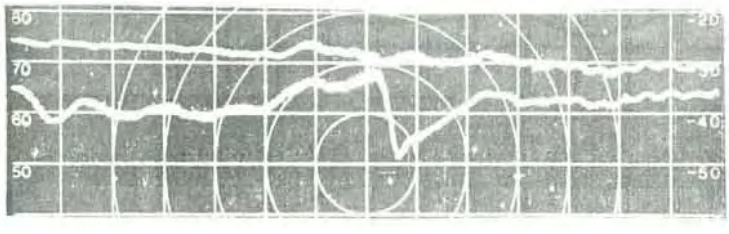

Fig. 5. Typical forward (upper) and reflected (lower) power at dipole inputs. 10 dB/div. Center frequency is 224 MHz.

The effect on the antenna performance is that the dipole impedance changes severly, see Fig. 3. The phase steering angle must be reduced to 21.3°. Then the average reflection is only 5%. The 600 Watt dummy loads in the line feed can tolerate 10% reflection which corresponds to $\theta=22.6^{\circ}$. However, the reflections from the dipoles vary much along the array for $\theta=22.6^{\circ}$, so that the dissipation in some loads may be larger than 600 Watt. The reason for the variation in return loss along the array is the coupling via T-junctions in the transmission line system.

I.6. Radio Source Measurements

The efficiency of the antenna was measured by means of the radio star Cassiopeia A. See Sec. III. The results are shown in Fig. 6. At broadside the antenna efficiencies are

$\eta = 0.69$ for horizontal pol. ($3300\ m^2$)
$\eta = 0.60$ for vertical pol. ($2900\ m^2$)

which gives

$\eta = 0.64$ for circular pol., i.e. $3100\ m^2$

This is higher than the efficiency of 0.60 which was guaranteed by MBB. The expected efficiency was 0.66 [9]. The measurement accuracy is about ±0.23 dB.

There is a gain discrepancy at 0.6 dB between horizontal and vertical polarization. 0.3 dB can be explained from aperture efficiency, blockage by diagonal struts and difference in insertion loss of transmission line system. See Sec. III.

For a phase steering angle of 21.3° the efficiency is close to the expected efficiency. The expected efficiency reduction is calculated in Sec. III as a function of scan angle. It is reduced because of increased spillover. For larger phase steering angles the efficiency is strongly reduced for vertical polarization due to the impedance mismatch in Fig. 3. See Fig. 6.

The maximum possible phase steering angle is 21.3° for vertical polarization

7 measured drift scans of Cas A are shown in Diagram 1-7. At broadside the sidelobe levels are higher than when the beam is phase steered. The reason is that at broadside the star drift through the beam in the east-west plane where the sidelobes are high, due to the uniform excitation of the line feed. For $\theta \neq 0$ the drift plane makes an angle with the east-west plane. The angle increases as a function of θ. The sidelobes are lower in any other plane through the antenna beam, and lowest in the north-south plane due to the tapered illumination of the reflector surface.

Truls Hansen (EISCAT) has made a computer program which determines the position of the antenna when a given radio source passes the beam, as a function of the phase steering angle θ_N, the elevation offset, and the mechanical scan plane offset. The program was used and worked satisfactorily.

An elevation offset of the antenna of $0.92^{\circ} \pm 0.07^{\circ}$
and a mechanical scan plane offset from the north-south plane of $0.55^{\circ} \pm 0.05^{\circ}$ west of north
was found from the star measurements. See Sec. III.

The calibration scale on the drift scans of Cas A is approximately "dB down from an antenna efficiency of 0.60". See Sec. III.4.

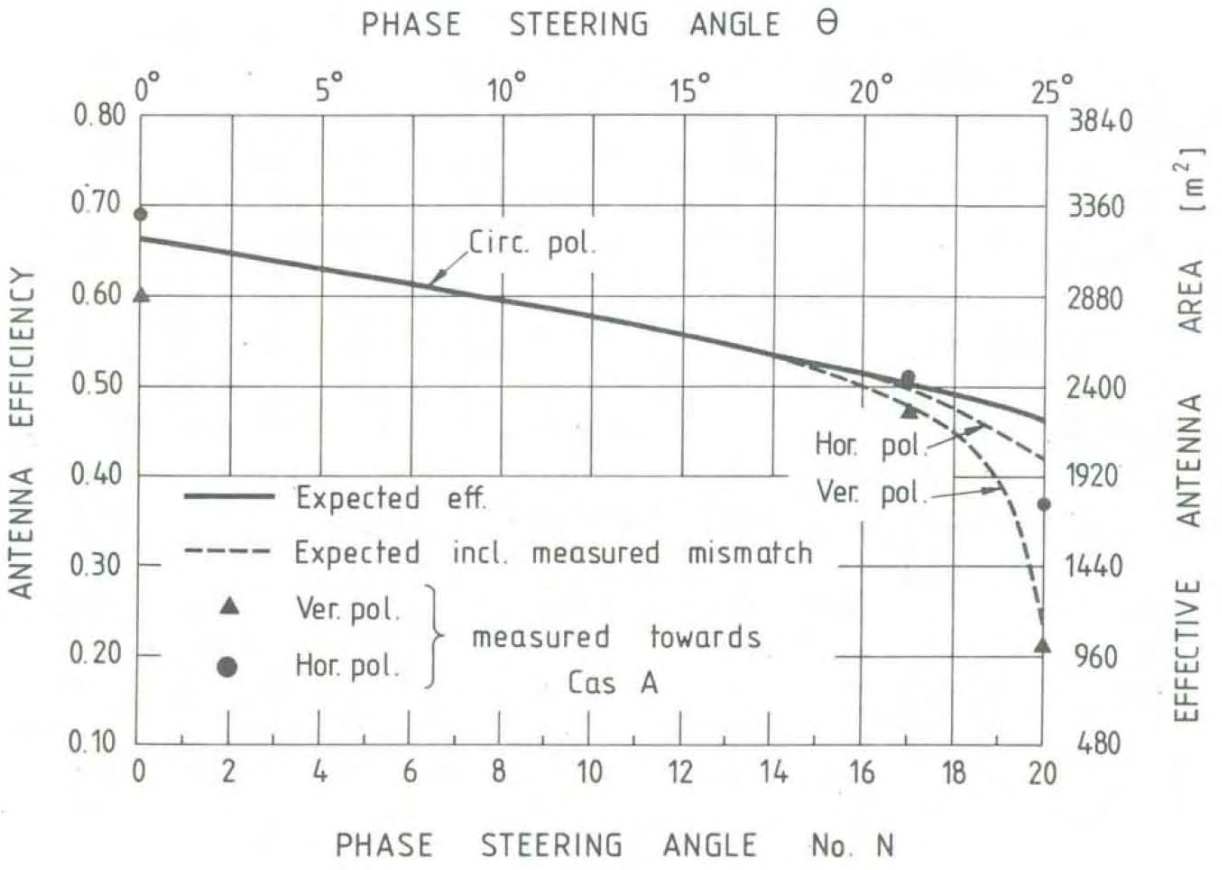

Fig. 6. Expected and measured efficiencies.

II. MEASUREMENTS OF REFLECTIONS AT DIPOLE INPUTS

When the linear array feed is phase steered, the active impedance of the dipoles change. The dipoles are matched at broadside. The reflections on the dipole inputs, therefore, increase as a function of phase steering angle. This reduces the gain according to

$$\eta_{imp} = 1 - 10^{-R/10} \qquad (1)$$

where R is the return loss in dB at the dipole inputs.

The last power dividers (i.e. closest to the dipoles) in the RF distribution system are 3 dB hybrids with 600 Watt loads on the dummy ports. When the feed is phase steered, part of the power reflected at the dipole inputs will add up at the dummy ports of the 3 dB hybrids and dissipate in the 600 Watt loads [9, p. 2.11]. The dissipated power is [9, Eq. (2.36)]

$$P_{dummy}(\theta_N) = 2(1-\eta_{imp}) \sin^2 (kd\sin\theta_N) \frac{P}{128} \qquad (2)$$

where θ_N is the phase steering angle, $d = 0.7\lambda_o$ is the element spacing in the linear array and p = 375 kW is the total transmitter power in each polarization. The rest of the reflected power is returned farther back in the distribution network. For $\theta \approx 21$ all the reflected power is dissipated, so that

$$R < 10 \text{ dB}$$

must be required to prevent damage of the 600W loads. This requirement turns out to limit the phase steering angle to $\theta_{max} = 21.3^o$.

The measurement setup is shown in Fig. 7. A calibrated measurement cable is inserted into the transmission line system in front of the dipole inputs. The measurement cable includes a directional coupler, which couples out the forward and reflected wave. The measurement cable has a length which allows the dipole to be exited with the right phase relative to the other

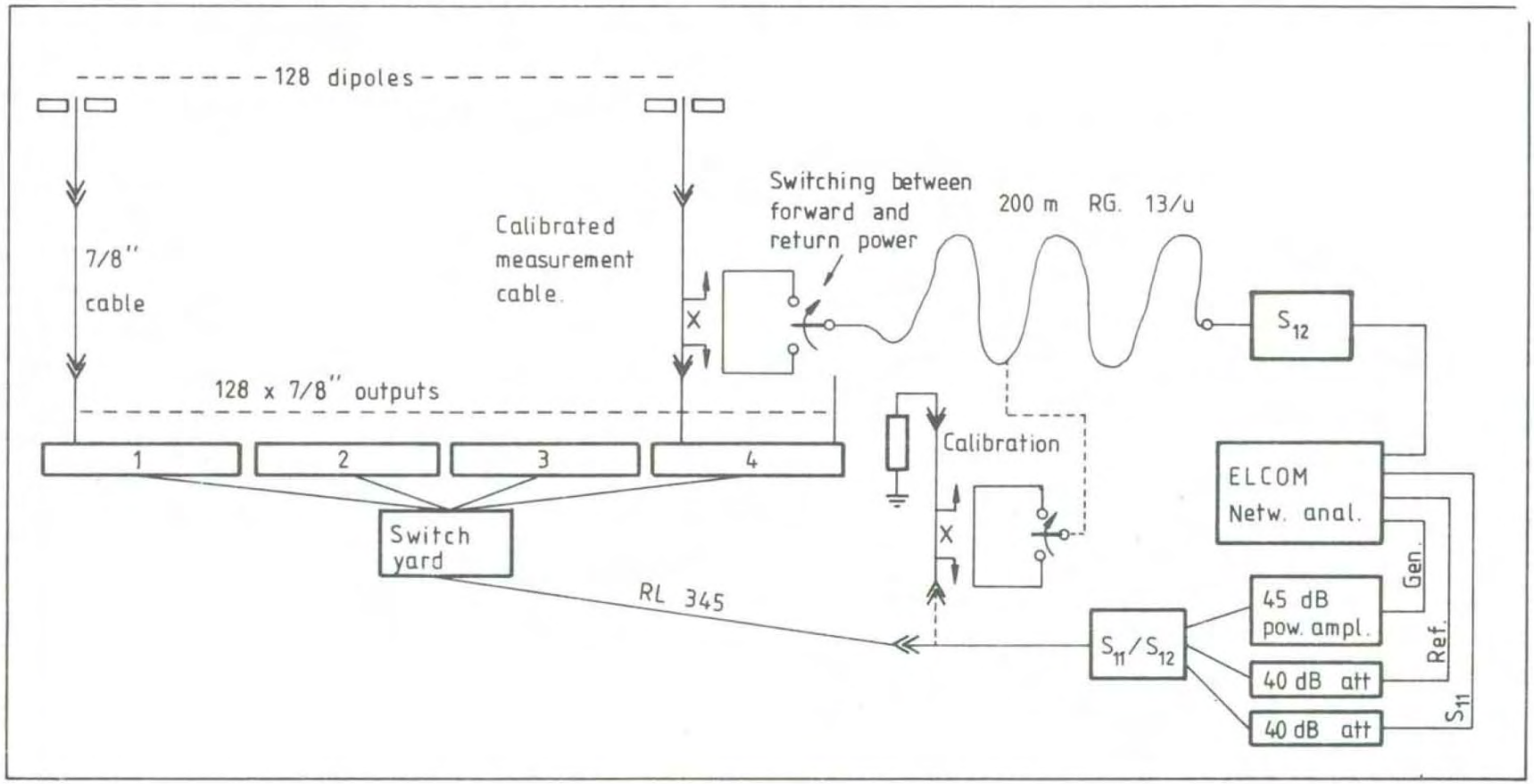

Fig. 7. Measurements of insertion loss and dipole reflections.
The calibrated measurement cable has the same electrical length as the 7/8" cable which it replaces.

dipoles. Thus, during measurements all dipoles are excited with the same amplitude and the correct phase. For details regarding the measurement setup see the measurement journal [11].

II.1 Broadside

The most important results measured at broadside are given here. More results are given in [11]. The reflections at the dipole inputs are measured on 8 dipoles. A typical measurement result is shown in Fig.5. Results for more dipoles are given in Table 3.

Table 3. Return loss at dipole inputs. Broadside. 224 MHz.

	Horizontal pol.		Vertical pol.	
Dipole No.	Return loss	η_{imp}	Return loss	η_{imp}
4	31 dB	0.999	26 dB	0.998
28	30 dB	"	31 dB	0.999
36	29 dB	"	31 dB	"
60	31 dB	"	28 dB	0.998
68	30 dB	"	29 dB	0.999
100	30 dB	"	29 dB	"
124	31 dB	"	29 dB	"
127	29 dB	"	28 dB	0.998

Table 3 shows that the dipoles are very well matched at broadside. The mean gain reduction due to mismatch is

$$\underline{\eta_{imp} \approx 0.999}$$

and the corresponding

$$VSWR \approx 1.07$$

for both polarizations.

II.2 Phase Steered

The same measurements are done with a phase steered beam. Some typical measurement curves are shown in Fig. 5. See also [11] and the tables below. A discussion of the results is given in Sec. I.5.

Table 4. Return loss at dipole inputs. 25.2° phase steering angle. 224 MHz.

Horizontal pol.			Vertical pol.		
Dipole No.	Return loss	η_{imp}	Dipole No.	Return loss	η_{imp}
1	17 dB	0.98	17	6.3 dB	0.766
11	17 dB	0.98	27	5.2 dB	0.698
58	16 dB	0.975	37	6.5 dB	0.776
74	16.5 dB	0.978	48	6.0 dB	0.749
84	15 dB	0.968	58	4.6 dB	0.653
94	15 dB	0.968	68	3.2 dB	0.521
104	16 dB	0.975	78	1.4 dB	0.276
105	18.2 dB	0.985	88	0.7 dB	0.149
115	18.6 dB	0.986	98	1.3 dB	0.259

The complete antenna was phase steered to 25.2°. See Table 4. The horizontal dipoles are well matched, giving (mean values)

$$\underline{\underline{\eta_{imp} \approx 0.97}}$$

The vertical dipoles are badly matched, giving

$$\underline{\underline{\eta_{imp} \approx 0.54}}$$

Eq. (2) gives the power dissipated in the dummy loads. The mean dissipated power in each load is obtained from Eq.(2) and the mean value of η_{imp}. We have

$P_{dummy}\ (25.2^{\circ})$ = 120 Watt for horizontal pol.

$P_{dummy}\ (25.2^{\circ})$ = 2500 Watt for vertical pol.

Therefore, in wiew of the 600w power rating on the loads, vertical polarization cannot be phase steered to 25.2°.

Table 5. Return loss at dipole inputs. 21.3° phase steering angle. 224 MHz.

Dipole No.	Horizontal pol. Return loss	η_{imp}	Vertical pol. Return loss	η_{imp}
1	14.8 dB	0.967	16.0 dB	0.975
17	25.8 dB	0.997	12.2 dB	0.940
36	24.6 dB	0.997	14.1 dB	0.961
51	25.0 dB	0.997	13.4 dB	0.954
70	23.4 dB	0.995	14.4 dB	0.964
93	24.6 dB	0.997	12.5 dB	0.944
107	26.2 dB	0.998	12.4 dB	0.943
119	21.4 dB	0.993	12.8 dB	0.948

The complete antenna was phase steered to 21.3°. Table 5 gives as before the following mean values

$\underline{\underline{\eta_{imp} \approx 0.99}}$ for horizontal pol.

$\underline{\underline{\eta_{imp} \approx 0.95}}$ for vertical pol.

and

P_{dummy} (21.3°) ≈ $\underline{\underline{60 \text{ Watt}}}$ for horizontal pol.

P_{dummy} (21.3°) ≈ $\underline{\underline{300 \text{ Watt}}}$ for vertical pol.

Thus, the antenna should work satisfactorily at 224 MHz with 21.3° phase steering angle.

Table 6. Return loss at dipole inputs. 22.6° and 23.9° phase steering angle. Vertical pol. only.

	22.6° phase steering angle		23.9° phase steering angle	
Dipole No.	Return loss	η_{imp}	Return loss	η_{imp}
68	13.2 dB	0.952	14.2 dB	0.962
78	10.0 dB	0.900	8.2 dB	0.849
88	8.5 dB	0.859	4.1 dB	0.611
98	11.9 dB	0.935	9.7 dB	0.893
106	11.2 dB	0.924	7.5 dB	0.822
116	9.5 dB	0.888	7.1 dB	0.805
126	14.4 dB	0.964	9.1 dB	0.877

The vertical dipoles along half the line feed were phased to 22.6° and 23.9°. Table 6 gives for vertical polarization.

$\underline{\underline{\eta_{imp} \approx 0.92}}$ for $\theta = 22.6^{\circ}$

$\underline{\underline{\eta_{imp} \approx 0.83}}$ for $\theta = 23.9^{\circ}$

and

$P_{dummy}\ (22.6^{\circ}) \approx \underline{\underline{500\ Watt}}$

$P_{dummy}\ (23.9^{\circ}) \approx \underline{\underline{1000\ Watt}}$

The mean dissipated power at 22.6° is less than 600 Watt. However, it is $\underline{\underline{\text{not advicable to phase steer to } 22.6^{\circ}}}$ because the dipole reflections vary much from dipole to dipole, so that the dissipated power may be too high in several loads.

III. RADIO STAR MEASUREMENTS

III.1. Available Radio Sources

The geographic coordinates of the EISCAT site at Ramfjordmoen are 69.583° North and 19.210° East. The VHF antenna is steerable in elevation in the North-south plane between 30° and 120° from north. The relation between the declination (γ) of a star, the elevation of the antenna measured from north (α), and the latitude of the position at the antenna (β), is approximately

$$\gamma = 90^{\circ} - \beta + \alpha \qquad (1)$$

Therefore, radio stars with declinations

$$\gamma > 39.6^{\circ}$$

when the antenna is near the horizontal 120° position, and

$$\gamma > 50.4^{\circ}$$

when the antenna is near the vertical 30° position, can be observed in transit through the main beam.

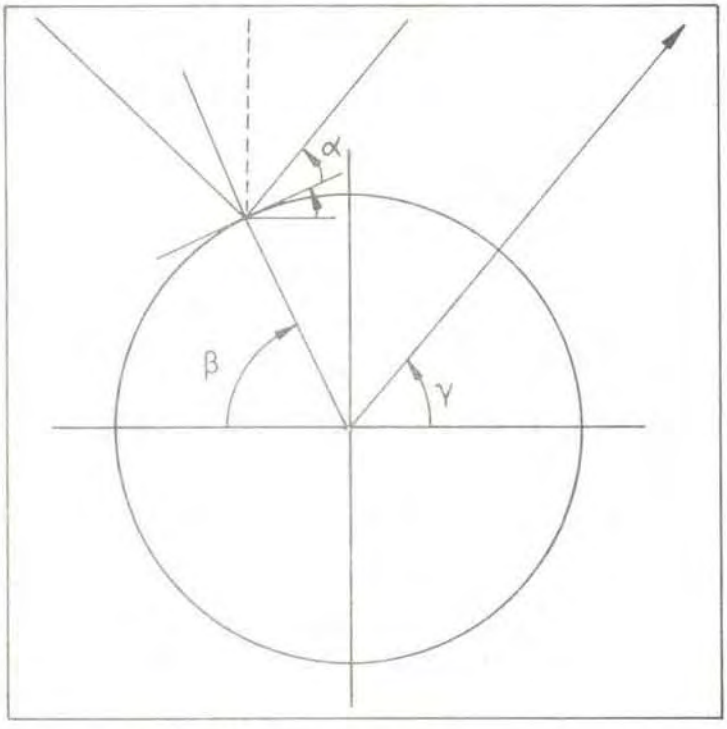

Fig. 8. Coordinates

If the beam is phase steered in the east-west plane the relations are more complicated. If the scan angle is θ_n measured from broadside, it is possible to show that the declination (γ) in the direction of the main beam becomes

$$\sin \gamma = \cos \theta_n \cos(\alpha-\beta) \qquad (2)$$

For the maximum scan angle $\theta_n = 25.2^o$ the lowest declination which is possible to reach is

$$\gamma = 35.2^o \qquad \text{for } \alpha = 120^o$$

$$\gamma = 44.2^o \qquad \text{for } \alpha = 30^o$$

Thus, only sources with a declination $\gamma > 35.2^o$ can be observed with the VHF antenna. Only sources with $\gamma > 44.2^o$ can be observed twice a day.

Phil Williams [5] has selected 31 sources from the Revised 3C catalogue which satisfy $\gamma > 34.6^o$, have a flux density larger than 20 Jy, have a "straight" spectrum (except Cyg A), and have an angular structure less than 0.13^o. The strongest of these sources are listed in Table 17 together with the most important characteristics.

The transit speed at equator is 4 min/^{o}. For a source with declination γ it becomes

$$t = \frac{4}{\cos \gamma} \quad [\text{min}/^o] \qquad (3)$$

SOURCE	Transit speed	Flux density	Equivalent noise temp. for A_{eff}=3200 m^2	Elevation measured from north	Appr. local time Early Dec.1979
CAS A	7.7 min/°	8730 Jy	10122 K	38.3°	06.16
CAS A	" "	"	"	100.9°	18.18
CYG A	5.3 min/°	7600 Jy	8820 K	118.9°	14.56
3C 10	9.1 min/°	127.5 Jy	148 K	84.4°	19.20
3C 10	" "	"	"	43.7°	07.20
3C 390.3	22.5 min/°	39.8 Jy	46 K	79.8°	13.35
3C 390.3	" "	"	"	59.3°	01.40

Table 7. . Radio sources. Reference of the flux densities is [3]. For Cas A see Sec. III.2

III.2. Flux Density of CAS A

The calibration of the gain depends on the accuracy by which the flux density of the available sources is known. The strongest and therefore most convenient source for gain calibrations is Cas A. The spectrum of Cas A has been studied by many authors recently, and is, therefore, quite accurately known. The flux density of Cas A n years after the flux density was F_0, as a function of the frequency f, is

$$F = F_0\left(\frac{f}{f_0}\right)^k [1 + B(f)]^n \qquad (4)$$

where k is called the spectral index, and B(f) is the decay rate. From [3] we have (Jy = Jansky = 10^{-26} Wm^{-2} Hz^{-1}) at epoch t_o = 1965.0

F_0 = 3181 ± 25 Jy, at f_o = 1 GHz

k = -0.792 ± 0.006

B(f) = -0.0097 ± 0.0005 + (0.00126 ± 0.00023) ln(f)

where f is the frequency in GHz.

The accuracy at 224 MHz in January 1980 becomes about 3% from the above uncertainties in F_o, k and B(f).

Thus, at 224 MHz in January 1980 we have

$$F = 8730 \pm 260 \text{ Jy} \quad \text{(i.e. } \pm 0.13 \text{ dB)}$$

This is quite different from for instance [3] which claims a different spectral index k = -0.765, giving F = 8180 Jy at 224 MHz. They differ by nearly 0.3 dB. However, [8] is a more recent publication and should therefore be more correct. ESA (the European Space Agency) also uses [8] as a reference for their gain calibrations [6]

The correction of the flux density for angular extension and atmospheric attenuation is negligible.

III.3. Measurement method

The efficiency of the antenna is found by measuring the receiver power when the sources is passing the beam. Here is referred to the received noise power P as an equivalent noise temperature T defined by

$$P = kTBG \qquad (1)$$

where k is Bolzmann's constant, B is the bandwidth, and G is the gain of the receiver system. In this way T is referred to the input of the preamplifier.

When the antenna is pointing towards the background sky, the different noise contributions are

$$T_1 = \eta_t \eta_{sp} T_{sky} + \eta_t (1-\eta_{sp}) T_a + (1-\eta_t) T_a + T_{rec} \qquad (2)$$

where η_t is the efficiency of the transmission line system. For 0.5 dB loss we have $\eta_t = 0.9$. η_{sp} is the spillover efficiency, $\eta_{sp} \approx 0.92$. T_{sky} is the noise temperature of the background sky, given approximately from Fig. 9. Including a spectral index of approximately -0.5 [2], we obtain 190 ± 10 K. T_a is the ambient temperature ($T_a \approx 270$ K), and T_{rec} is the noise temperature of the receiver. ($T_{rec} \approx 160$K). Thus, the expected value of T_1 is

$$T_1 \approx 360 \text{ K}$$

When the antenna is pointing towards the source, the received noise increases by

$$P = \frac{1}{2} G \eta_a A F B \qquad (3)$$

where A is the aperture area of the antenna, and η_a is the antenna

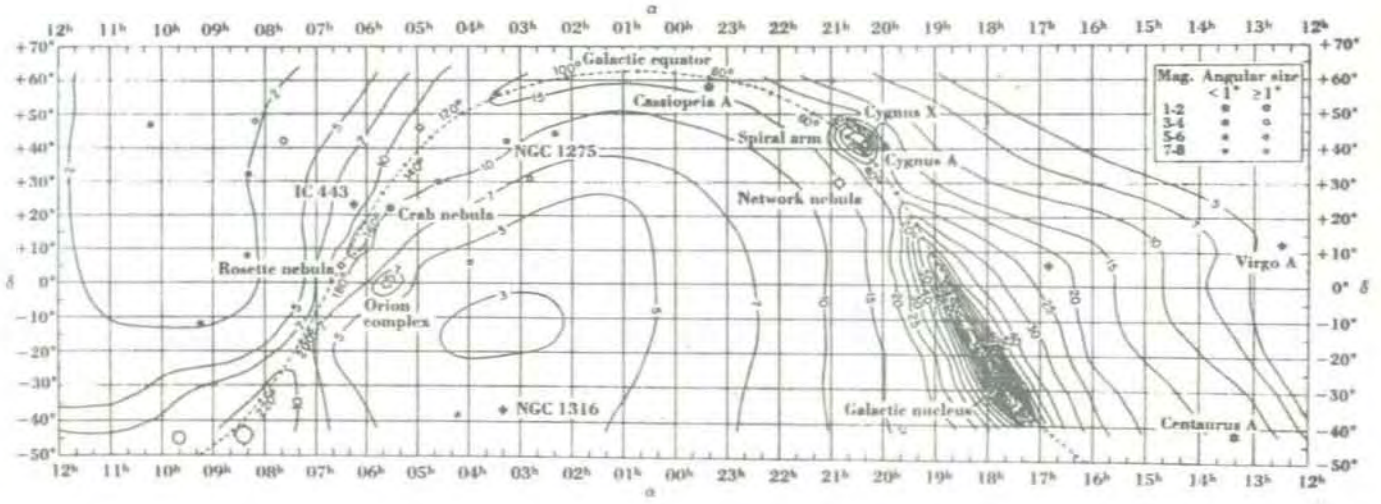

Fig. 9. Radio sky at 250 MHz [2, p.296]. The contours are in units of 6 K above 80 K. Thus, countour 15 is at temperature 15 x 6 K + 80 K = 170 K.

efficiency including η_t. The factor $\frac{1}{2}$ is due to the reception of one polarization only. Introducing the equivalent noise temperature defined by Eq. (1) we obtain for the source

$$T_{source} = \frac{1}{2k} \eta_a A F \tag{4}$$

The total received noise temperature is

$$T_2 = T_{source} + T_1 \tag{5}$$

which is about 10 000 K for Cas A.

Hence, by measuring T_2 and T_1 it is possible to evaluate the antenna efficiency η_a. It becomes

$$\eta_a = \frac{2k}{AF} (T_2 - T_1) \tag{6}$$

For A = 4800 m^2 and F = 8730 Jy we have, including a correction factor for measuring at an offset frequency f,

$$\eta_a = 0.659 \cdot 10^{-4} (T_2 - T_1) \left(\frac{f}{224}\right)^{-0.792} \tag{7}$$

III.4. Calibration

The accuracy by which the antenna efficiency can be calculated depends on the accuracy of the flux density, which for Cas A was ± 0.13 dB, and the accuracy by which T_2 and T_1 can be measured.

The calibration setup used in the measurements is shown in Fig. 10. A logaritmic receiver was used.

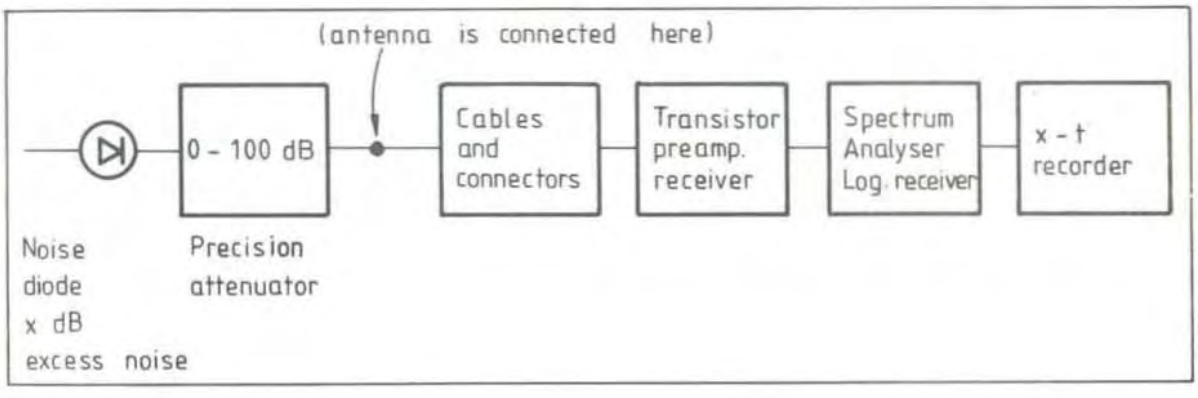

Fig. 10. Calibration setup

The total noise temperature measured in the system in Fig. 10 as a function of the attenuation a [dB] of the precision attenuator is

$$T_{cal}(a) = 10^{\frac{x-a-0.4}{10}} T_0 + (1-10^{-\frac{a}{10}}) T_a + T_{rec} \qquad (8)$$

where T_0 = 290 K, and T_a = 270 K for outdoor environments in winter. x[dB] is the excess noise of the noise diode used. The number 0.4 is the insertion loss of the attenuator.

The measurement of T_2 and T_1 corresponds to two readings a_2 and a_1 on the attenuator. We have

$$T_2 - T_1 = T_{cal}(a_2) - T_{cal}(a_1)$$

$$= \left[10^{\frac{x-0.4}{10}} T_0 - T_a\right]\left[10^{-\frac{a_2}{10}} - 10^{-\frac{a_1}{10}}\right] \qquad (9)$$

Using a calibrated noise diode with x = 15.6 dB excess noise, the result is

$$10 \log \left[(T_2 - T_1)/T_0\right] \approx 15.08 - a_2 \quad \text{for } a_2 - a_1 >> 20$$

The antenna efficiency in dB becomes therefore from Eq. (7)

$$\underline{10 \log \eta_a \approx \left[-2.11 - a_2 - 7.92 \log \left(\frac{f}{224}\right)\right] \text{ dB}} \qquad (10)$$

Eq(10) is only valid if $a_2 - a_1 >> 20$. In the measurements on Cas A a reading a_1 corresponding to the background noise level T_1 cannot be made because

$$T_1 < T_{cal}(\infty)$$

In Sec. II.3 is found that $T_1 \approx 200$ K + T_{rec} near Cas A and from Eq. (8) $T_{cal}(\infty) = T_a + T_{rec} = 270$ K + T_{rec}. In this case Eq.(10) is only valid if

$$T_2 >> T_1 \approx 200 \text{ K} + T_{rec}$$

which gives

$$a_2 < 20 \text{ dB}$$

The guaranteed performance (guaranteed by manufacturer) of the antenna is $A_{eff} = 2900$ m^2, corresponding to $a_2 = 0.08$ dB. Thus, any reading of the received noise of Cas A which satisfies $a_2 < 0.08$ dB $\approx$ 0 dB is satisfactory.

Therefore, for drift patterns obtained by Cas A, the calibration scale (a) is directly giving the beam pattern in dB down from specified gain when a < 20 dB.

The expected performance is A_{eff} = 3250 m^2, corresponding to a_2 = -0.42 dB, for circular polarization [9].

The frequency correction on the flux desity of Cas A when the measurements are done on another frequency than 224 MHz is very small. See Eg. (10). When the measurements are made at 230 MHz, the correction is -0.09 dB.

The disadvantage with this setup is that calibrations must be done before the transit of the star, so that the calibrations are very sensitive to gain instabilities in the receiver. That was a problem with the logaritmic receiver in the spectrum analyzer which had a periodic (12 minutes) variation of ±0.4 dB for the measurements done in December 1979. In February and March 1980 it was possible to increase the long time stability to ±0.1 dB. Thus, the total measurement accuracy was (instability + accuracy of flux density of Cas A)

in Dec. 1979	± 0.53 dB
in Febr./March 1980	± 0.23 dB

The accuracy is also reduced by scintillations of received noise signal.

III.5.Result

18 drift scans of radio sources were measured in Dec. 1979, and 20 in February/March 1980. They are all found in the measurement journal [10]. Six of them are included in this report. Diagram No.7 was measured by Kristen Folkestad and Truls Hansen in January 1980. It is included because the scintillations are small. The scintillations turned out to be a problem in most of the drift scans. They varied from day to day, causing the received noise level from Cas A to oscillate with up to ± 3 dB with periodes less then 1 second (rapid scintillations) and up to 20 seconds (slow scintillations).

Broadside measurements:

The elevation offset of the antenna was found by moving the antenna up and down when the star drifted through the beam. The result is shown in Table 8.

Table 8. Elevation offset

Patt.No.	Date	Star	Sec.or pol.	El.of star	Ant.pos for star max.	Elev. offset
79.II	3.Dec.	Cas A	3-4	38.3^{o}	$39.3^{o}\pm0.1^{o}$	$1.0^{o}\pm 0.1^{o}$
79.III	3.Dec.	Cas A	1-2	100.9^{o}	101.8^{o}	0.9^{0}
79.IX	7.Dec.	Cyg A	1-2	118.9^{o}	119.75^{o}	0.85^{o}
79.VI	5.Dec	Cas A	too much scintillation			
80.VIII	5.March	Cas A	too much scintillation			

Conclusion: elevation offset ~ $0.92^{o} \pm 0.07^{o}$

The time of transit t_{real} turned out to be different from the computed time of transit t_{comp}. The difference was due to a deviation of the mechanical tilt plane of the antenna from the north-south plane. However, the line of intersection of the two planes seems to coincide with the zenit direction. The deviation $\Delta\varphi$ is calculated as

$$\Delta\varphi = \frac{t_{comp.} - t_{real}}{4 \text{ min./o}} \cdot \frac{\cos \gamma}{\cos \alpha}$$

where α is the elevation, and γ the declination, and $\Delta\varphi$ is positive towards west from north. The result is shown in Table 9.

Table 9. Deviation of mechanical tilt plane from north-south plane.

Patt.No.	Date	Star	Sec.or pol.	Elevation of star	Deviation in deg.West of North
79.III	3 Dec.	Cas A	1-2	100.9^{o}	$0.7^{o} \pm 0.2^{o}$
79.IX	7 Dec.	Cyg A	1-2	118.9^{o}	$0.5^{o} \pm 0.1^{o}$
80.XVIII	19 March	Cas A	HOR and VER	38.3^{o}	0.57^{o}
80.XIX	20 March	Cyg A	HOR and VER	118.9^{o}	0.59^{o}
80.XX	20 March	Cas A	switching	100.9^{o}	$0.5^{o} \pm 0.8^{o}$

Conclusion: Deviation ~ $0.55^{o} \pm 0.05^{o}$ west of north

The effective aperture area is measured as explained in Sec.III.3 and III.4. The frequency in some cases had to be tuned away from 224 MHz due to interference with other users of the frequency band. The results are shown in Table 10.

Table 10. Gain at broadside (N=0) using Cas A. A_{eff} is calculated from Eqs. (7) and (10).

Patt.No.	Date	Antenna position	Freq.	Pol.	a_2	A_{eff}
79.VII	6 Dec.	39.3°	230 MHz	HOR	-0.5 dB	3240 m^2
79.X	7 Dec.	101.9°	228 MHz	HOR	-0.9 dB	3580 m^2
79.XII	8 Dec.	101.9°	228 MHz	HOR	-0.5 dB	3270 m^2
79.XIII	9 Dec.	39.3°	228 MHz	HOR	-0.7 dB	3420 m^2
79.XV	10 Dec.	39.3°	228 MHz	HOR	-0.6 dB	3340 m^2
79.XVI	11 Dec.	39.3°	228 MHz	HOR	-0.3 dB	3120 m^2
79.VIII	6 Dec.	101.9°	230 MHz	VER	0 dB	2890 m^2
80.I	28 Febr.	39.4°	230 MHz	VER	~ 0 dB	2890 m^2
80.II	29 Febr.	39.4°	230 MHz	VER	~ 0 dB	2890 m^2
80.III	3 March	39.4°	230 MHz	VER	~ 0 dB	2890 m^2

Mean, horizontal pol. $A_{eff} = 3330 \pm 240\ m^2$
i.e. antenna efficiency $\eta_a = 0.69$

Mean, vertical pol. $A_{eff} = 2890 \pm 210\ m^2$
i.e. antenna efficiency $\eta_a = 0.60$

The accuracy is assumed to be ± 0.23 dB as discussed in Sec. II.4. There seems to be a gain difference between horizontal and vertical polarization of approximately 0.6 dB.

In pattern No. 80.IV, 80.V, 80 XVIII, 80.XIX and 80.XX in [10] the receiver is switched between horizontal and vertical polarization during drift of Cas A and Cyg A. Scintillations caused problems, but a gain difference of about 0.5 dB between horizontal and vertical polarization seems to be present.

Phase-steered beam:

The gain was also measured when the line feed was phase-steered to 21.3° and 25.2° West of north. The results are shown in Table 11.

Table 11. Gain with phase-steered antenna towards Cas A.

Patt.No.	Date	Antenna position	Freq.	Pol.	Phase-steering angle	a_2
80.VIII	March 5	51.3°	224 MHz	VER	25.2°	4.5 dB
80.IX	March 6	90.1°	224 MHz	HOR	25.2°	~2.5 dB
80.XI	March 6	51.3°	225 MHz	HOR	25.2°	2 dB
80.XII	March 7	-	224 MHz	VER	25.2°	5 dB
80.XIII	March 17	94°	224 MHz	VER	21.3°	1.2 dB
80.XIX	March 17	47°	224 MHz	HOR	21.3°	0.8 dB
80.XV	March 18	94°	224 MHz	HOR	21.3°	0.8 dB
"	"	"	"	VER	21.3°	1.2 dB

Average the different measurements of a_2, use Eq. (10) and get for horizontal polarization.

$$\text{at } 21.3^{\circ} \quad A_{eff} \approx 2450 \text{ m}^2, \text{ i.e. } \eta_a = 0.51$$

$$\text{at } 25.2^{\circ} \quad A_{eff} \approx 1800 \text{ m}^2, \text{ i.e. } \eta_a = 0.37$$

and for vertical polarization

$$\text{at } 21.3^{\circ} \quad A_{eff} = 2250 \text{ m}^2, \text{ i.e. } \eta_a = 0.47$$

$$\text{at } 25.2^{\circ} \quad A_{eff} = 1000 \text{ m}^2, \text{ i.e. } \eta_a = 0.21$$

The gain reduction at 21.3° is caused by the increased spillover over the west edge, the reduced illuminated reflector area near the other edge, and the projected aperture area.

The reason for the gain difference may be explained as follows. The aperture efficiency (spillover included) for horizontal polarization is 0.1 dB higher than for vertical polarization [9, p. 6.22].

The insertion loss of the transmission line system is 0.04 dB larger for vertical pol. [12]. And the blockage by the diagonal struts in the aperture is larger for vertical polarization. The width of the struts is 30 cm or 0.22 λ. The total blockage area of 8 struts over half the aperture width is then

$$A_b = 8 \times 0.30 \times 20 \text{ m}^2 = 48 \text{ m}^2$$

For a strut width of 0.22 λ the induced field ratio is for vertical polarization, i.e. the polarization parallel with the struts, equal to about 2.3, whereas it for horizontal polarization is only 0.8 [13]. The blockage efficiency becomes

$$\text{for horisontal pol.} \quad \eta_b = (1 - \frac{48 \cdot 0.8}{4800})^2 = 0.98, \text{ i.e. } -0.07 \text{ dB}$$

$$\text{for vertical pol.} \quad \eta_b = (1 - \frac{48 \cdot 2.5}{4800})^2 = 0.95, \text{ i.e. } -0.22 \text{ dB}$$

Thus a difference of 0.15 dB

The sum of all three teoretical contributions give 0.3 dB gain difference. The measured difference is about 0.6 dB. This discrepancy may be due to the measurement accuracy or to the accuracy of the computations of the aperture efficiency.

The spillover efficiency becomes

$$\eta_{sp} = 1 - \frac{F_m}{L} \tan\theta$$

where L = 120 m is the length of the line feed, and F_m = 30 m is the mean distance from the line feed to the reflector surface. The illuminated reflector area is reduced by the same amount, so that

$$\eta_{red} = \eta_{sp}$$

The projected aperture area cause a reduction in efficiency

$$\eta_{pr.} = \cos\theta$$

Thus,

$$\eta_{21.3^o} = \eta_{sp}\ \eta_{red}\ \eta_{pr} = \underline{\underline{0.76}} \quad \text{for } \theta = 21.3^o$$

$$\eta_{25.2^o} = \underline{\underline{0.70}} \quad \text{for } \theta = 25.2^o$$

If we multiply the measured aperture efficiencies at broadside with 0.76 we get quite exactly the corresponding aperture efficiencies at 21.3^o. Thus, the gain reduction is as expected at 21.3^o.

At 25.2^o the reduction in antenna efficiency is much larger than 0.70. That is due to mismatch of the dipole impedances.

See Sec. I.5 and II.2.

References

[1] A.J. Freiby. P.D. Batelaan, and D.A. Bathker, "Radio source gain standards for large aperture antenna calibrations", Paper at IEEE 1978 Antennas and Propagation International Symposium, Proceedings

[2] J.D. Kraus, Radio Astronomy, New York: McGraw-Hill.

[3] K.I. Kellermann and I.I.K Pauliny-Toth, "The spectra of radio sources in the revised 3C catalogue", The Astrophysical Journal, Vol. 157, July 1969.

[4] Per-Simon Kildal, "Discrete phase steering by permuting precut phase cables", EISCAT Technical Note 78/6, October 1978.

[5] Phil Williams, "Observations of standard radio sources at 224 MHz using the VHF telescope at Tromsø", Private communications to Tor Hagfors.

[6] "G/T measurements of INTELSAT standard earth stations", ESA Document, October 1979.

[7] R.M. Price, "Radiometer Fundamentals", in Astrophysics Radio telescopes, M.L.Meeks, Ed. New York: Academic, 1976.

[8] W.A.Dent, H.D.Aller and E.T.Olsen, "The evolution of the radio spectrum of Cassiopeia A", The Astrophysical Journal, Vol. 188, Febr. 1974, L11 - L13.

[9] Per-Simon Kildal, "Feeder elements for the EISCAT VHF parabolic cylinder antenna", EISCAT Technical Note 78/8, October 1978.

[10] Per-Simon Kildal, "Gain measurements using radio stars." Measurement journal, EISCAT, Tromsø, Norway.

[11] Per-Simon Kildal, "Additional RF-tests: Reflection measurements", Measurement journal, EISCAT, Tromsø, Norway.

[12] G.Schroer, "RF-acceptance tests ", Test journal, EISCAT, Tromsø, Norway.

[13] W.V.T. Rusch, "Forward scattering from cylinders of triangular cross section", IEEE Trans. Ant. Propagat., Vol AP-26, No.6, Nov. 1978, pp. 849-850.

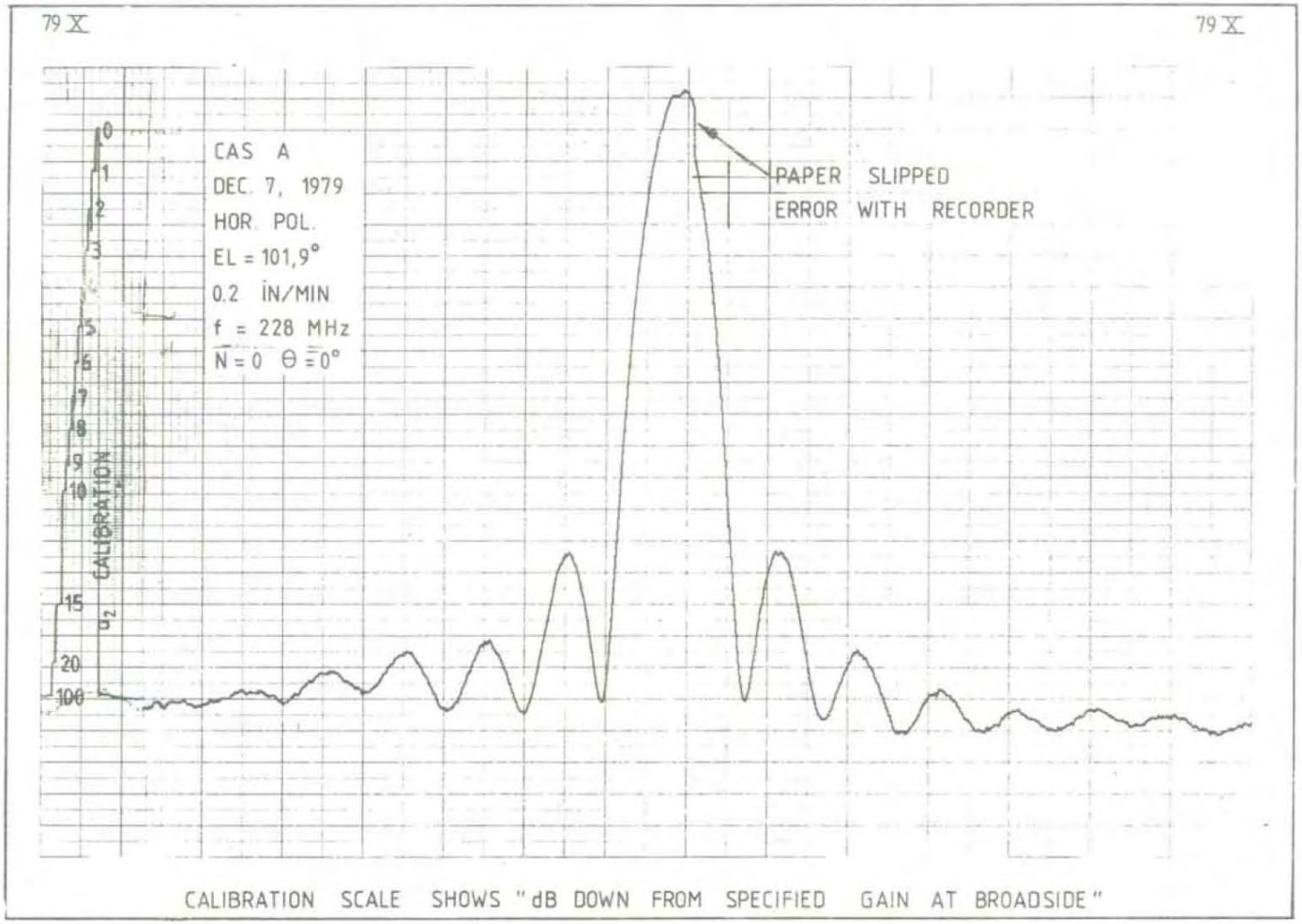

Diagram 1. Horizontal polarization. Broadside. Pattern No. 79 X. Calibration scale shows "dB down from specified gain at broadside"

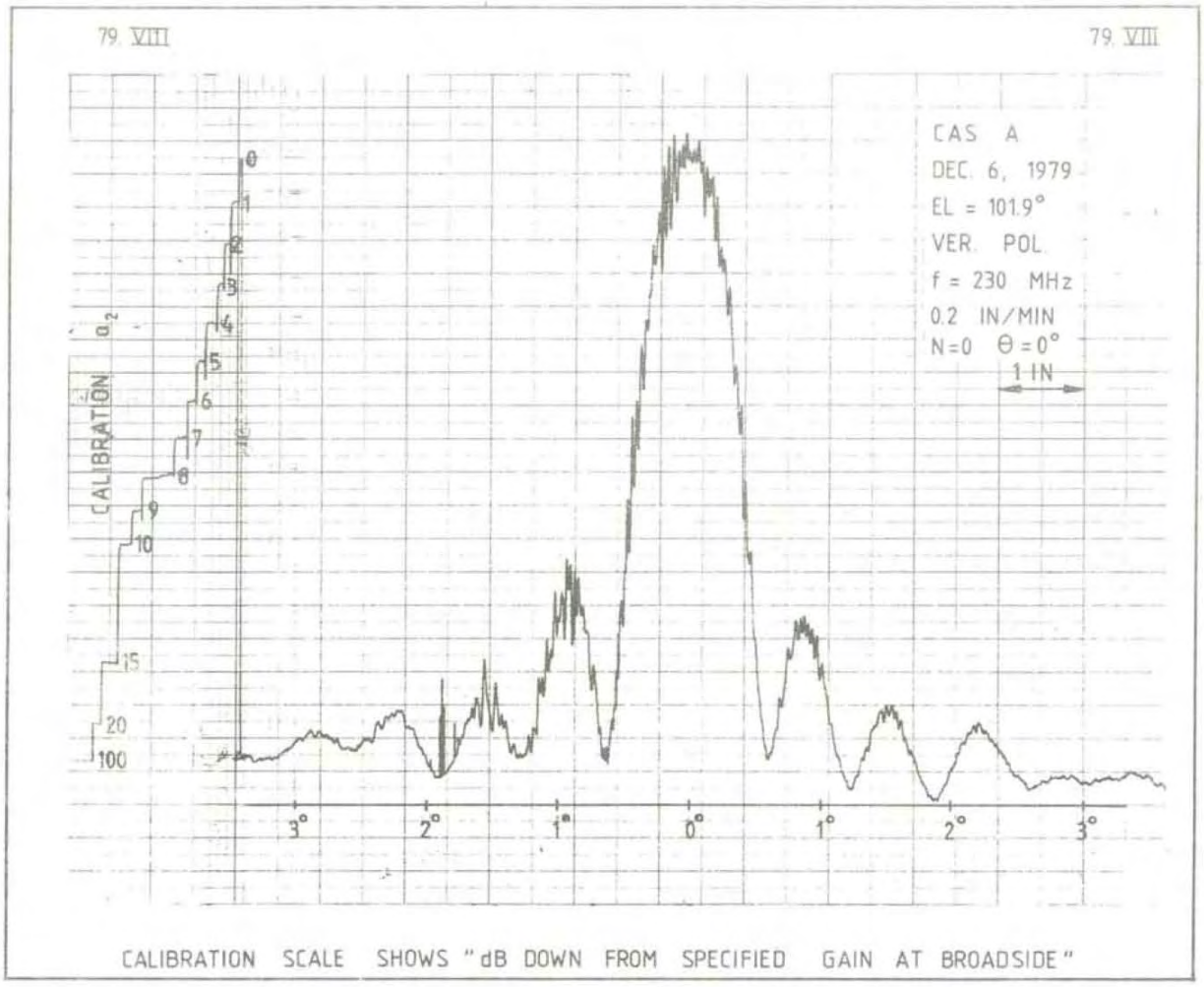

Diagram 2. Vertical polarization. Broadside. Pattern No. 79 VIII. Calibration scale shows "dB down from specified gain".

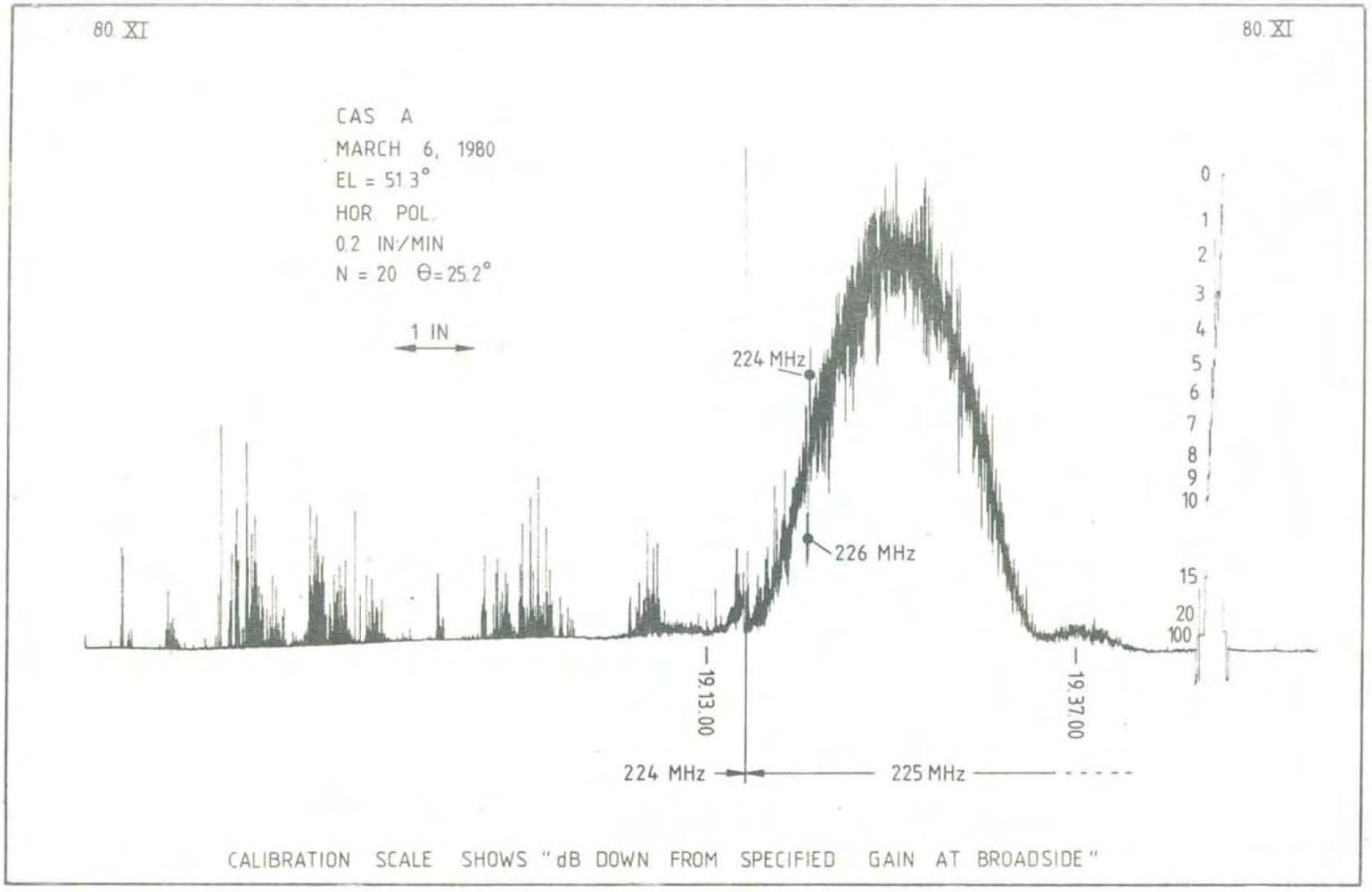

Diagram 3. Horizontal polarization. Phase steered to 25.2°, i.e. N = 20. Position of beam is a function of frequency as expected. Calibration scale shows "dB down from specified gain at broadside".

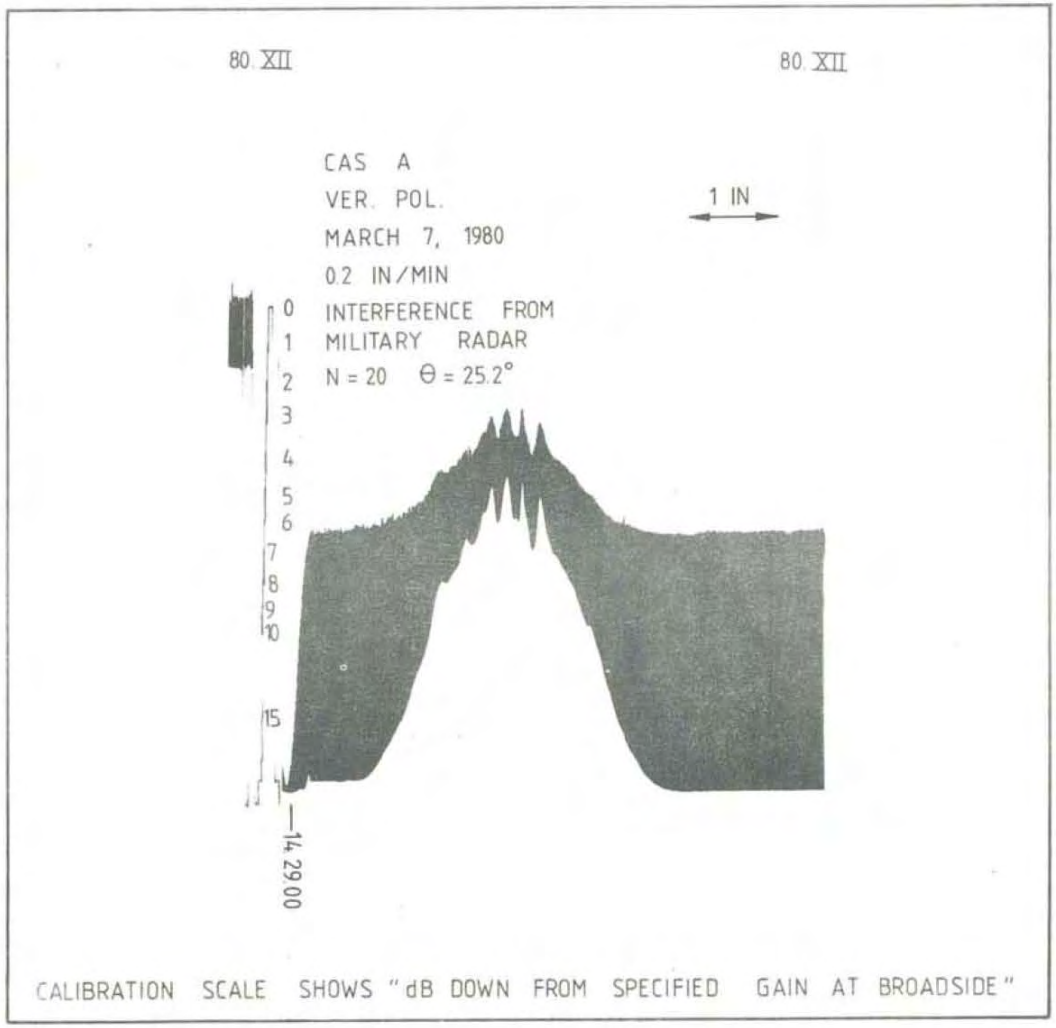

Diagram 4. Vertical polarization. Phase steered to 25.2°, i.e. N = 20. Large interference with military radar with pulse repetition frequency about 1 Hz. Calibration scale shows "dB down from specified gain at broadside".

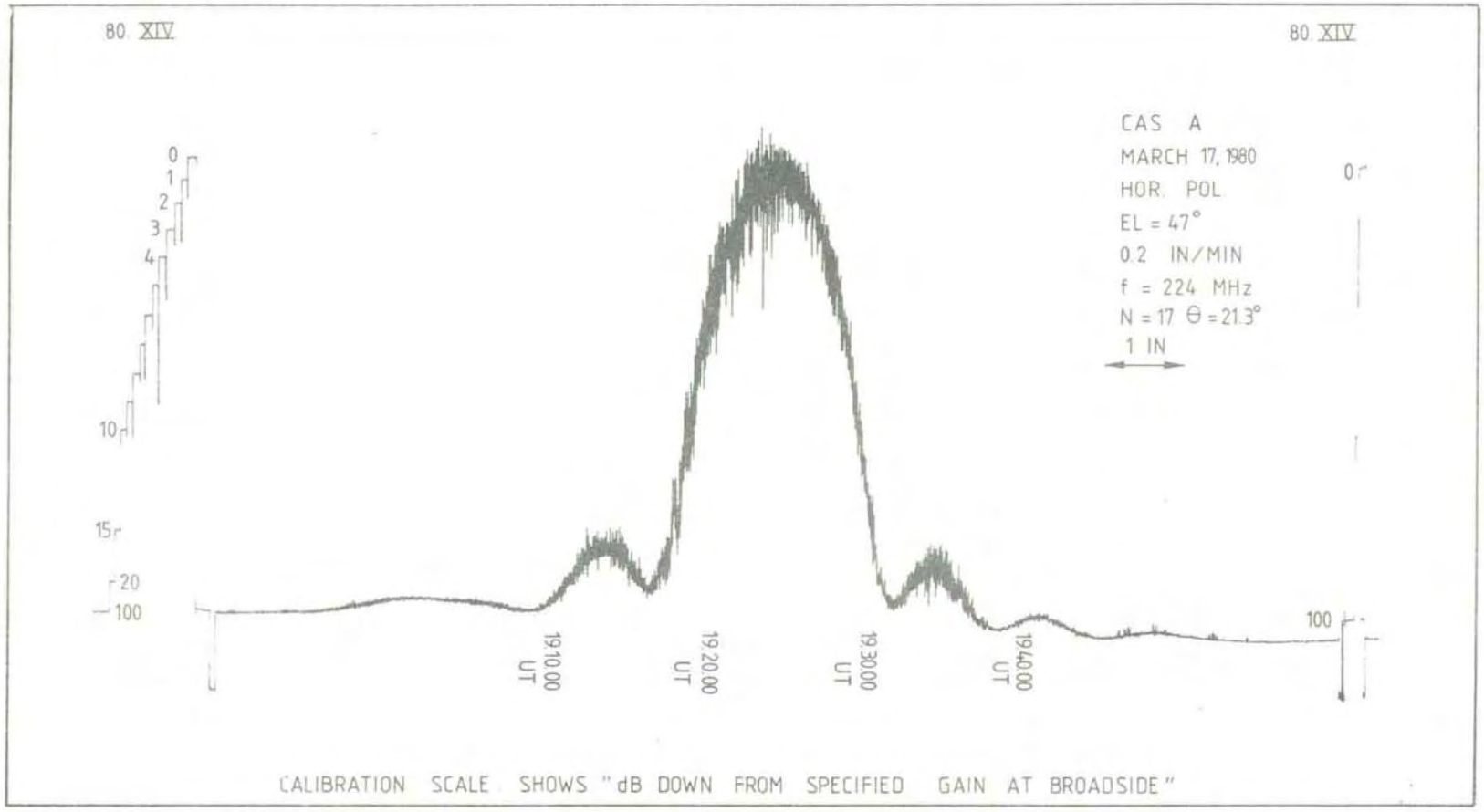

Diagram 5. Horizontal polarization. Phase steered to 21.3°, i.e. N = 17. Rapid scintillations. Calibration scale shows "dB down from specified gain at broadside".

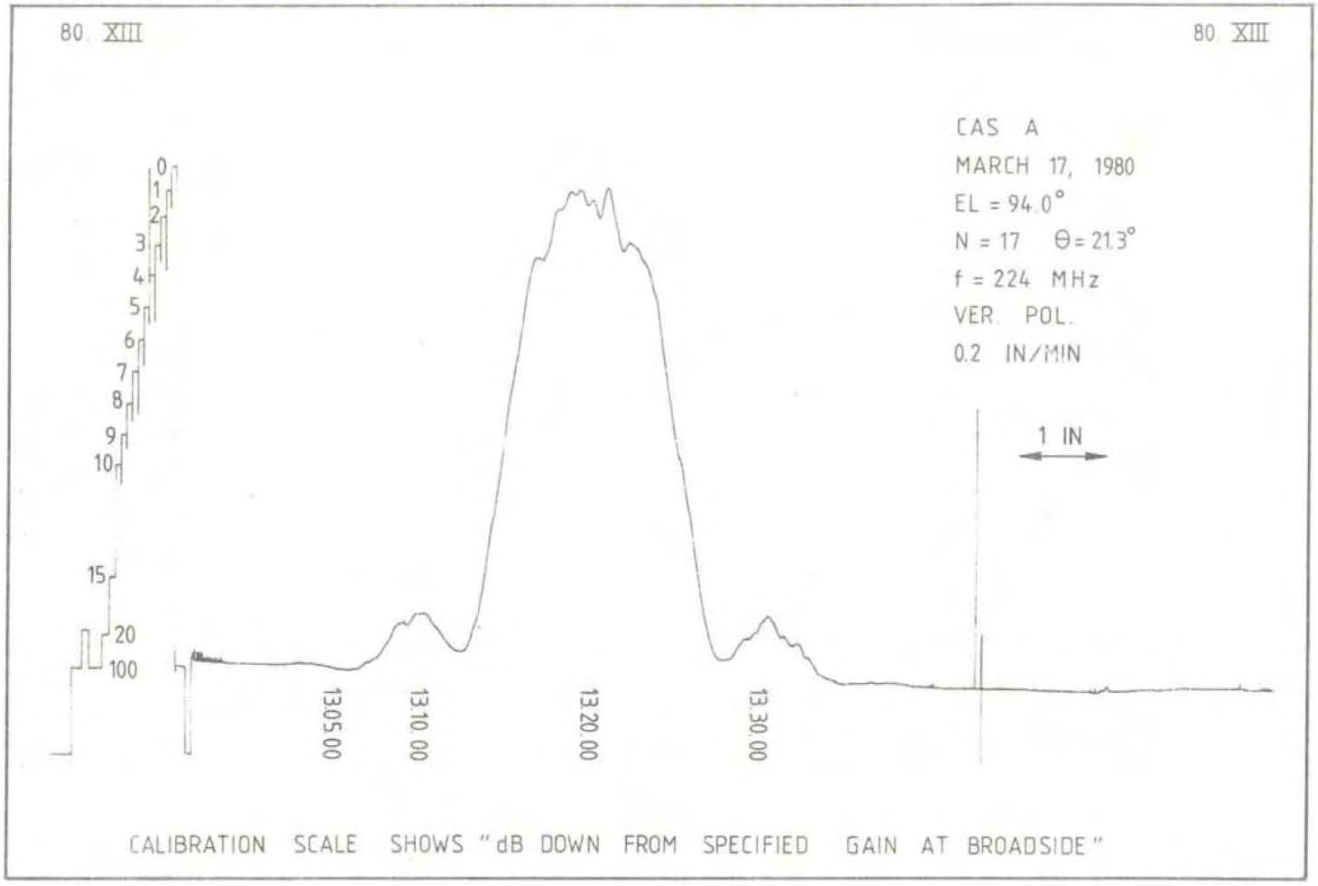

Diagram 6. Vertical polarization. Phase steered to 21.3°, i.e. N = 17.
Slow scientillations. Pattern No. 80. XIII.
Calibration scale shows "dB down from specified gain at broadside".

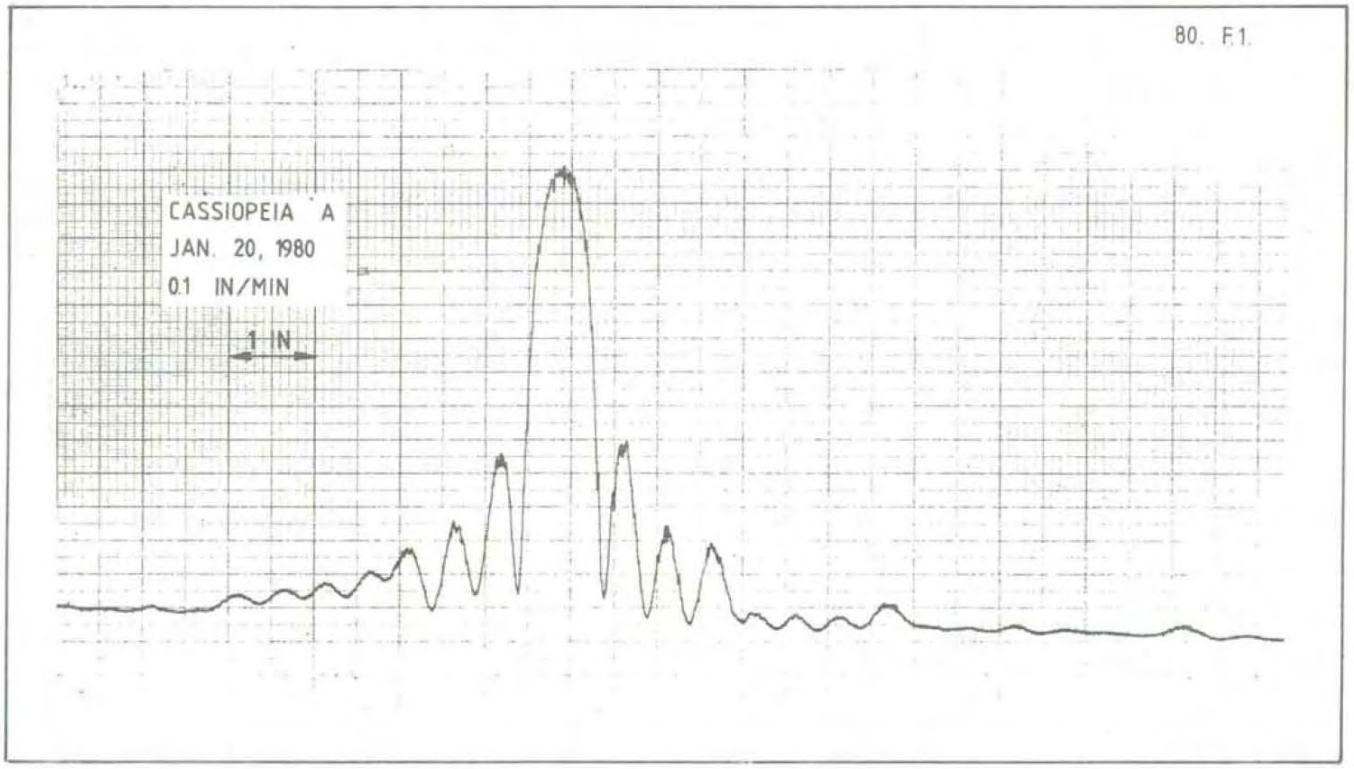

Diagram 7. Broadside. Very small scintillations. Pattern No. 80.F.1.

EISCAT publications

F. du Castel, O. Holt, B. Hultqvist, H. Kohl and M. Tiuri:
A European Incoherent Scatter Facility in the Auroral Zone (EISCAT).
A Feasibility Study ("The Green Report") June 1971. (Out of print).

O. Bratteng and A. Haug:
Model Ionosphere at High Latitude, EISCAT Feasibility Study, Report No. 9.
The Auroral Observatory, Tromsö July 1971. (Out of print).

A European Incoherent Scatter Facility in the Auroral Zone, UHF System and Organization ("The Yellow Report"), June 1974.

EISCAT Annual Report 1976.(Out of print).

P.S. Kildal and T. Hagfors:
Balance between investment in reflector and feed in the VHF cylindrical antenna.
EISCAT Technical Notes No. 77/1, 1977.

T. Hagfors:
Least mean square fitting of data to physical models.
EISCAT Technical Notes No. 78/2, 1978.

T. Hagfors:
The effect of ice on an antenna reflector.
EISCAT Technical Notes No. 78/3, 1978.

T. Hagfors:
The bandwidth of a linear phased array with stepped delay corrections.
EISCAT Technical Notes No. 78/4, 1978.

Data Group meeting in Kiruna, Sweden, 18-20 Jan. 1978
EISCAT Meetings No. 78/1, 1978

EISCAT Annual Report 1977

H-J. Alker:
Measurement principles in the EISCAT system
EISCAT Technical Notes No. 78/5, 1978

EISCAT Data Group meeting in Tromsö, Norway 30-31 May, 1978
EISCAT Meetings No. 78/2, 1978.

P-S. Kildal:
Discrete phase steering by permuting precut phase cables.
EISCAT Technical Notes No. 78/6, 1978

EISCAT UHF antenna acceptance test.
EISCAT Technical Notes No. 78/7, 1978.

P-S. Kildal:
Feeder elements for the EISCAT VHF parabolic cylinder antenna.
EISCAT Technical Notes No. 78/8, 1978.

H-J. Alker:
Program CORRSIM: System for program development and software simulation of EISCAT digital correlator, User's Manual.
EISCAT Technical Notes No. 79/9, 1979.

H-J. Alker:
Instruction manual for EISCAT digital correlator.
EISCAT Technical Notes No. 79/10, 1979

H-J. Alker:
A programmable correlator module for the EISCAT radar system.
EISCAT Technical Notes No. 79/11, 1979.

T. Ho and H-J. Alker:
Scientific programming of the EISCAT digital correlator.
EISCAT Technical Notes No. 79/12, 1979.